HHS Public Access

Author manuscript

Integr Biol (Camb). Author manuscript; available in PMC 2021 August 26.

Published in final edited form as:

Integr Biol (Camb). 2011 November ; 3(11): 1063–1070. doi:10.1039/c1ib00061f.

Vascular Smooth Muscle Contractility Depends on Cell Shape

Patrick W. Alford[1,2], **Alexander P. Nesmith**[1], **Johannes N. Seywerd**[1], **Anna Grosberg**[1], **Kevin Kit Parker**[1]

[1]Disease Biophysics Group, Harvard Stem Cell Institute, Wyss Institute of Biologically Inspired Engineering, School of Engineering and Applied Sciences, Harvard University, Cambridge, MA 02138

[2]Current Address: Department of Biomedical Engineering, University of Minnesota-Twin Cities, Minneapolis, MN 55455

Abstract

The physiologic role of smooth muscle structure in defining arterial function is poorly understood. We aimed to elucidate the relationship between vascular smooth muscle architecture and functional contractile output. Using microcontact printing and muscular thin film technology, we engineered *in vitro* vascular tissues with strictly defined geometries and tested their contractile function. In all tissues, vascular smooth muscle cells (VSMCs) were highly aligned with *in vivo*-like spindle architecture, and contracted physiologically in response to stimulation with endothelin-1. However, tissues wherein the VSMCs were forced into exaggerated spindle elongation exerted significantly greater contraction force per unit cross-sectional area than those with smaller aspect ratios. Moreover, this increased contraction did not occur in conjunction with an increase in traditionally measured contractile phenotype markers. These results suggest that cellular architecture within vascular tissues plays a significant role in conferring tissue function and that, in some systems, traditional phenotype characterization is not sufficient to define a functionally contractile population of VSMCs.

Graphical Abstract

Corresponding author: Kevin Kit Parker, 29 Oxford St (Rm 322A), Cambridge, MA 02138, Phone: (617) 495-2850, Fax: (617) 495-9837, kkparker@seas.harvard.edu.

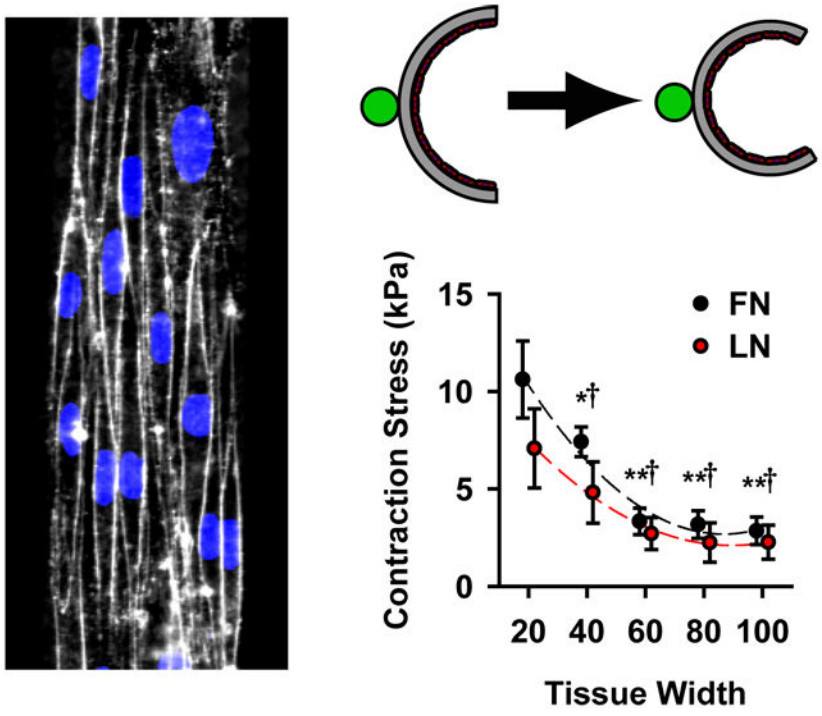

Vascular smooth muscle function is measured in vitro and shown to be determined by cellulr and tissue architecture

INTRODUCTION

There is a fine interplay between structure and function in biological systems. However, it is often unclear whether function is derived from structure or if structure follows from functional requirements. Recent results indicate that cellular and tissue structure, enforced by constrained boundary conditions, can confer directed function of cell processes such as apoptosis[1], lamellipodia extension[2], cytoskeletal and focal adhesion organization[3–5] and electrical conductance[6]. However, the relationship between vascular smooth muscle structure and contraction, the primary function of vascular tissue, is relatively unstudied.

Vascular smooth muscle cells (VSMCs) have markedly different structures in different arteries[7]. In all healthy arteries, VSMCs have a characteristic spindle shape; however, in elastic arteries such as the aorta, the spindle is less pronounced, while in muscular arteries the spindle is elongated and well defined[7]. This elongated muscular geometry may function to facilitate tone modulation in muscular arteries, where dynamic response to blood flow rate[8, 9] and pressure[10, 11] are more important. However, to date this relationship has not been demonstrated.

Understanding the relationship between structure and function in VSMCs is complicated by the fact that, under different conditions, they can play two distinct physiological roles[12]. In a healthy mature artery, VSMCs' primary function is maintenance of vascular tone. However, following injury, VSMCs switch their phenotype; losing contractility, becoming proliferative

and migratory, and producing more extracellular matrix (ECM)[13]. This phenotype switching plays a role in a number of vascular disorders such as hypertension[14], restenosis[15] and vasospasm[16]. Elucidating the many triggers of this switching between contractile and synthetic VSMCs is an area of current interest[12, 17].

The traditional methods for identifying VSMC phenotype are measurement of protein or RNA expression of standard contractile markers, cell migration persistence, or cell proliferation rate. Using these approaches, it has been shown that VSMC phenotype can be modulated by a number of factors, including ECM composition[18–20], substrate rigidity[21], mechanical stimulation[22, 23], growth factor stimulation[24, 25] and cell or tissue geometry[26, 27]. Most prior VSMC phenotype studies have been done *in vitro*, on glass or polystyrene substrates, so it has not been possible to measure contractile function associated with expression changes.

We hypothesized that tissue structure directly affects contractility in VSMCs. To address this hypothesis we utilized techniques previously developed in our laboratory for high fidelity tissue engineering[28–30], where a 2D muscle tissue can be engineered with cellular shape control, the contractility measured, and the lysates collected for expression analysis. We find that an elongated spindle-like cell shape strongly correlates with contractile function of VSMCs, even in the absence of concurrent changes in contractile markers. This result suggests that cell geometry plays a significant role in muscle function and that traditional measures of VSMC phenotype may not be sufficient for predicting functional behavior in vascular tissue.

RESULTS

Controlling Tissue Architecture with Soft Lithography

We hypothesized that vascular tissue architecture would regulate contractile strength. We reasoned that we could control the geometry of cell shapes within a vascular smooth muscle tissue by assembling multicellular VSM fibers on long bands of extracellular matrix, where the band width could be varied to constrain VSMC geometry. Tissues were constructed as 20, 40, 60, 80 and 100 μm wide lines separated by 100 μm gaps (Fig 1A). This approach allowed us to control three key predictors of VSMC contractility: cell architecture, cell-cell contact density and extracellular signaling cues.

We previously observed that in anisotropic tissues consisting of VSMCs, individual cells' short axes were greater than 20 μm[29]. Thus, by limiting lateral migration, the 20 μm wide patterning forced the cells within the micropatterned tissue into a thinner more exaggerated spindle-like conformation, characteristic of contractile cells. Moreover, the thinner tissues (20, 40 μm) were limited to only one to three cells spanning their width, while the wider tissues had increased parallel registration of cells (Fig 1A). Increased cell-cell contact has been shown to induce greater expression of contractile markers[31], suggesting that the wider tissues should be more contractile. Thus, the tissue micropatterning provided multiple geometric cues for VSMC contractility.

Cell-ECM interactions regulate a wide range of physiological phenomena ranging from cell migration[32] to differentiation[33]. In VSMCs, differential ECM cues have been shown to drive phenotypic expression, with laminin (LN) inducing a more contractile phenotype than fibronectin (FN)[18]. Here, the cells were seeded in a serum-free defined medium and patterned with either FN or LN, to elucidate the functional response to ECM-integrin signaling.

Micropatterned tissue thickness was measured using confocal microscopy of phalloidin stained f-actin (Fig 1B). Local thickness was not uniform within a given tissue (Fig 1C), however, the average thickness of the tissue was unchanged between different tissue widths, when ECM substrate was controlled for (Fig 1D). The result of this tissue engineering protocol was repeatable, highly organized tissues with defined geometries and multiple independently controllable phenotypic cues.

Vascular Tissue Structure and Contractile Strength

To measure the contractility of the micropatterned tissues, we employed vascular muscular thin films (vMTFs)[29, 30], which are flexible two-layer biohybrids composed of a layer of polydimethylsiloxane (PDMS) and a layer of micropatterned VSMCs (Fig 2A). Contraction in the VSMC layer bends the PDMS resulting in a measurable curvature of the construct (Fig 2B,C) that can be used to calculate the tissue stress, or force per cross-sectional area (see Methods and Alford et al[29] for details). To determine the dose-response behavior of the tissues, we serially stimulated the vMTFs with increasing doses of the vasoconstrictor endothelin-1 (ET-1) (500 pM, 5 nM, 50 nM, 500 nM) (Fig2D). All tissue patterns demonstrated typical sigmoidal dose-response behaviors in response to this stimulus (Fig 3A,B). Controlling for cell coverage, we found that the thinner tissues contract significantly more than the wider tissues (Fig 3A,C) and that tissues patterned on fibronectin generated slightly greater ET-1 induced contraction stress than those patterned on laminin (Fig 3B,C).

Following ET-1 stimulation, the vMTFs were treated with 100 μM HA-1077, a rho-associated kinase (ROCK) inhibitor, sufficient to inhibit all contraction in the constructs (see Fig 2D). By comparing the initial stress to the ROCK inhibited stress, we calculated the basal contractile tone of the micropatterned tissue. Pattern dependent basal tone mirrored ET-1 induced contraction stress with the 20 μm wide tissues exhibiting significantly greater stress than wider lines (Fig 3D). These results demonstrate that VSMC functional behavior can be modulated by tissue architecture.

Subcellular Alignment in Micropatterned Tissue

We asked whether differences in cytoskeletal organization would indicate the functional differences in the different tissue architectures. To address this question, we measured alignment of f-actin and nuclei in the micropatterned tissues, using histochemical staining (Fig 4A,B). We measured actin orientation using a method based on fingerprint identification algorithms[4] (Fig 4B,C), and quantified alignment (Fig 4D) by calculating the orientational order parameter (OOP)[34] of the actin fibers. For all tissues, the OOP was greater than 0.95, where 1.0 represents perfect alignment and 0 is random organization (Fig 4E). We also quantified nuclear organization by measuring the orientation of the major axis

of the ellipse that best fit the DAPI stained nuclei[35] (Fig 4F,G). OOP of nuclear organization was above 0.95 for all tissue with no significant differences between groups (Fig 4H). These data suggest that the cells and their cytoskeletons are highly aligned in all tissue patterns, thus variable alignment of contractile mechanisms is likely not the source of the differential contractility between the different tissue architectures.

Cell Shape and Functional Contractile Output

Though there were no differences in actin organization, cellular geometry and organization within the tissue varied in the different tissue widths (Fig 5A). We asked whether cell shape was correlated with the contractility of our micropatterned vascular tissues. Mature contractile VSMCs have a characteristic spindle shape, while synthetic cells tend to be pleomorphic[12]. We asked if the spindle shape itself optimizes contractile functionality. Using live membrane and nuclear staining (Fig 5A), we noted that cell aspect ratio is correlated with nuclear eccentricity (Fig 5B), consistent with previous findings[35], allowing us to use nuclear eccentricity as an indicator of cell geometry. In tissues patterned on both fibronectin and laminin, the thinner tissues had higher nuclear eccentricities, with 20 μm and 40 μm wide tissues statistically different from 60–100 μm wide tissues (Fig 5C). Moreover, nuclear eccentricity strongly correlated with vMTF measured stress of both ET-1 induced contraction (Fig 5D) and basal contractile tone (Fig 5E). These results suggest that functional contractile output of VSMCs is dependent on cellular architecture.

Tissue Structure and Phenotype Expression

During development, VSMCs undergo a switch from a synthetic (motile and proliferative) phenotype to a mature contractile phenotype[12]. Additionally, VMSCs can revert to a synthetic phenotype following injury or disease[36] or in culture[37]. We measured the protein expression of two prominent contractile phenotype markers[13], smooth muscle myosin heavy chain (SM-MHC) and smoothelin, in our patterned tissues to determine if phenotype switching accounted for the elevated contraction stress in the thinner tissues (Fig 6A). Similar techniques for controlling cell geometry have been shown to affect phenotypic behavior in VSMCs[26, 27, 31].

Consistent with previous studies[18], we found that tissues patterned on laminin expressed SM-MHC and smoothelin at greater levels than those on fibronectin (Fig 6B,C). We also found that the markers were elevated in the wider tissues, consistent with previous observations that increased cell-cell contacts induce greater contractile phenotype expression[31] (Fig 6B,C). It is normally assumed that SM-MHC and smoothelin expression are predictive of a contractile phenotype[12, 13]. However, there was not a positive correlation between contractile marker expression and ET-1 induced contraction stress (Fig 6D) or basal contractile tone (Fig 6E). This data suggests that the observed increase in contractility in the thinner tissues is not due to phenotypic switching, as customarily measured.

DISCUSSION

Recent work has suggested that often cellular and tissue-level functional behavior can be conferred by structural organization[1–6]. Here, we used micropatterned vascular tissue with

enforced structural characteristics, due to constrained boundary conditions, to study the relationship between cell shape and contractile output in vascular smooth muscle. We found that the elongated spindle shape, characteristic of VSMCs in muscular arteries, strongly correlates with greater contractility. Previous researchers have shown that VSMC alignment, with the resultant spindle architecture, can induce an increase in traditionally measured contractile phenotype markers, compared to unaligned cells[27, 31]. Our result suggests that increased cell elongation within an aligned tissue can maximize contractile output, even in the absence of concurrent increase in contractile mechanism markers.

A number of factors contribute to VSMC phenotypic determination, including mechanical environment[21–23] and biochemical stimulation[24, 25]. ECM substrate composition has also been shown to have a marked effect on phenotype expression *in vitro*. Collagen I substrates provide mixed phenotypic cues, depending whether the collagen is fibrillar or monomeric[38], laminin upregulates contractile marker expression[18, 19], and fibronectin induces a more synthetic phenotype[20]. Here, we patterned tissues using fibronectin or laminin as a substrate. Consistent with previous findings, we found increased expression of contractile phenotype markers in tissues constructed on laminin, compared to fibronectin. However, this relationship was not reflected in the functional contraction of the tissues. This result suggests a more fundamental question about vascular smooth muscle: what is the definition of a contractile phenotype, proteomics or function?

Traditionally, in the absence of a robust functional assay, *in vitro* studies of VSMCs have relied on expression of contractile apparatus-associated markers to define phenotype switching, with SM-MHC and smoothelin being two of the most robust markers[13]. The vMTF assay presented here allows direct measurement of functional output of *in vitro* VSMCs. Using this assay, we found that for varying tissue architecture, contractile output correlated poorly with SM-MHC and smoothelin expression, but did correlate well with cell shape and nuclear morphology. This result suggests that phenotype marker measurement is not sufficient for describing a VSMC as functionally contractile and additional assays, such as the vMTF assay, should be used in conjunction with these measurements to fully describe VSMC phenotype.

It has been suggested that both vessel-level geometry[39, 40] and spatial distributions of artery constituents[41, 42] (VSMCs, collagen and elastin) can affect artery mechanics. It stands to reason that smaller scale geometric variation within the vessel could play a similar role. VSMCs in many arteries are separated into discrete lamellae by concentric elastin sheets[7, 43]. In the experiments reported here, the tissue shape restriction due to micropatterning may be mimicking the lateral constraint imposed by lamellar elastin. The increased functional contraction in our thinner micropatterned tissues suggests that this constraint may play a role as a tissue-level geometric cue for mechanical regulation in arteries *in vivo*.

Our finding that cell shape is correlated with tissue contractility suggests an important role for cell shape in arterial function. As mentioned previously, cellular morphology varies as a function of arterial function[7]. Studies with other cell types suggest that cell shape is an important regulator of gene expression and cell function[1, 44], and in the heart, changes

in striated muscle cell morphology have been associated with contractile function and dysfunction[45, 46]. Our results suggest that remodeling of VSMC shape could contribute to unique functionalities within the vascular system. It is notable that we find nuclear morphology correlates with both cell shape and contractile function. The cytoskeleton is interconnected with the nuclear lamina[47, 48], and extracellular stresses have been shown to actively deform the nucleus[49]. Additionally, internally generated contractile stress induces increased nuclear eccentricity in cardiac myocytes[35]. It has been proposed that nuclear deformation by cytoskeletal forces plays a key role in mechanotransduction[48, 50]. The sum of these reports and our own data suggest that the nuclear mechanics may have an important role in determining cell contractile function.

In this study we show that controlled vascular tissue structure can be employed to direct functional behavior, a finding that is particularly relevant in vascular tissue engineering, where the assembly of small diameter arterial replacements has been a goal of the field for nearly two decades[51]. Though a great deal of research has been done to address this need[52–54], mechanically viable and functionally active engineered small arteries are still elusive. Our data suggest that, in addition to replicating the chemical and mechanical environment of artery development, providing organizational guidance cues that force replication of healthy *in vivo* VSMC cellular architecture could provide mechanical functionality for implantable small artery grafts.

METHODS

Sample Preparation

Microcontact Printing.—Extracellular matrix (ECM) proteins fibronectin (BD Biosciences, Sparks, MD) or laminin (Invitrogen, Carlsbad, CA) were microcontact printed onto the polydimethylsiloxane (PDMS) (Sylgard 184, Dow Corning, Midland, MI) substrate, as previously published[29]. Briefly, the ECM was incubated on a PDMS stamp with microscale raised features for 1 hour and blown dry. The MTF substrate was UV-ozone treated for 8 minutes, after which the dried ECM coated stamp was placed in contact with it, transferring the ECM to the substrate. The sample was then incubated in 1% Pluronics F127 for 5 min. When seeded, cells were constrained to the ECM patterned portion of the substrate, guiding organization into aligned tissues. VSMC tissues were constructed with widths of 20, 40, 60, 80 and 100 μm, with individual tissue fibres separated by gaps of 100 μm.

Muscular Thin Films.—Vascular muscular thin films were constructed as previously published[28]. First, the thermosensitive polymer poly(N-isopropylacrylamide) (PIPAAm) (Polysciences, Warrington, PA) was spin coated onto a 25 mm glass coverslip, then PDMS doped with 0.2 μm diameter fluorospheres (Invitrogen, Carlsbad, CA) was spin coated on top of the PIPAAm layer. The construct was cured at 65°C for a minimum of 4 hours. For imaging and western blotting experiments substrates were made without the PIPAAm layer, with PDMS directly spin coated onto the glass.

Cell Culture

Human umbilical artery vascular smooth muscle cells (VSMCs) were purchased from Lonza (Walkersville, MD) at passage 3 and cultured in growth medium consisting of M199 culture medium (GIBCO, Invitrogen, Carlsbad, CA) supplemented with 10% fetal bovine serum (Invitrogen), 10 mM HEPES (GIBCO, Invitrogen, Carlsbad, CA), 3.5 g/L glucose, 2mg/L vitamin B-12, 50 U/ml penicillin and 50 U/mL streptomycin (GIBCO). All experiments were performed at passage 5–7.

VSMCs were seeded in a defined medium[55] of M199, 10 mM HEPES, 3.5 g/L glucose, 2mg/L vitamin B12, 50 U/mL penicillin, 50 U/mL streptomycin, 0.2% bovine serum albumin, 10 ng/mL pletlet-derived growth factor, 10 ng/mL epidermal growth factor, 20 ng/mL insulin-like growth factor, and 5 ug/mL transferring (all growth factors from Sigma Aldrich, St Louis, MO). Cells were seeded at 10,000 cells/cm^2, creating a confluent tissue, and incubated in growth medium for 24 hours. Defined seeding medium was then replaced with a growth factor free medium of M199, 10 mM HEPES, 3.5 g/L glucose, 2mg/L vitamin B12, 50 U/mL penicillin and 50 U/mL streptomycin to induce a contractile phenotype[56], for 24 hours prior to contractility or biochemistry experiments.

vMTF Stress Measurement

Vascular muscular thin film tissue stresses were calculated as previously published[29]. Briefly, prior to the experiment, the tissues are cultured at 37°C. At the time of the experiment, the tissue and PDMS layers of the construct are cut into strips and the medium is allowed to cool below 32°C, dissolving the PIPAAm layer. The free-floating vMTFs were then transferred to a separate dish of 37°C Tyrode's solution where they were attached to polytetrafluoroethylene (PTFE) coated posts in a conformation where their radii of curvature could be observed[29]. The vMTFs were serially stimulated with 500 pM ET-1, 5 nM ET-1, 50 nM ET-1, and 500 nM ET-1 followed by 100 μM HA-1077 (Sigma-Aldrich, St Louis, MO). The radius of curvature was measured under a stereomicroscope (Ziess Lumar V12, Carl Zeiss, Oberkochen, GER) under fluorescent illumination. The tissue force necessary to bend the film to the observed curvature was calculated by assuming that the vMTF is a two-layer beam with one passive layer (PDMS) and one active layer (VSMCs)[29] (Fig 2A). For the stress calculation, the cross-sectional area of the tissue was determined from the tissue height (Fig 1 C,D) and the fractional substrate coverage, where

$$\%\,coverage = \frac{\%\,patterned}{\%\,patterned + \%\,unpatterned}$$

The stress calculation is independent of film width, as long as the film is sufficiently wide that the % coverage equation above is approximately valid. To assure this, all vMTFs were cut with a minimum width of 2 mm. The serial stimulation allows measurement of the dose response curve to ET-1 stimulation and the basal contractile tone, i.e. the contraction stress prior to any stimulation. FN and LN contractility results were compared using an ANOVA test, with pairwise comparisons performed using a Tukey test.

PDMS layer and tissue layer thickness are needed to calculate vMTF stress[28, 29]. The PDMS thickness of MTF substrates fabricated at the same time as those used in the experiments was measured using stylus profilometery (Dektak 6M, Veeco Instruments, Inc., Plainview, NY) and assumed to be the same as those used. Tissue thickness was measured using confocal microscopy. F-actin was stained with Alexfluor 488 phalloidin and local thickness was measured using the z-plane locations of f-actin filaments. The tissue thickness was taken as the average local thickness in the tissue covered regions. The cross-sectional area used to calculate the tissue stress was the measured tissue thickness x tissue width, as dictated by the micropatterning.

Histochemistry

Micropatterned tissues were stained for F-actin (phalloidin) and nuclei (DAPI). Actin orientation was calculated from phalloidin staining[4]. Nuclear orientation and eccentricity were calculated by fitting an ellipse to each individual nucleus and calculating the orientation of the major axis of the ellipse[35] and its eccentricity, defined as $e = \sqrt{1 - \left(\frac{minor\ axis\ length}{major\ axis\ length}\right)^2}$. Actin and nuclear orientation were quantified for ten images in a single tissue and the total orientational order parameter[34] was calculated for each tissue. Non-normal eccentricity data was compared using a Kruskal-Wallis ANOVA on ranks test and pairwise comparisons were done using Dunn's method.

To quantify cell shape within the patterned tissue samples, tissues were live stained with (50 ug/mL) DAPI for 15 minutes at 37°C followed by (3 μM) Di-8-ANEPPS (Invitrogen, Carlsbad, CA) for 2 minutes in Tyrodes solution with Pluronic F-127 (20% solution in DMSO at 4°C). Samples were then rinsed with Tyrodes solution and immediately imaged using a Ziess 5-Live (Carl Zeiss, Oberkochen, GER) line scanning confocal microscope. Cell aspect ratio was measured manually from the membrane stain, using ImageJ.

Western Blotting

RIPA buffer contained 50 mM Tris, pH 8.0, 150 mM NaCl, 0.1% SDS, 1.0% NP-40, 0.5% sodium deoxycholate and protease inhibitor cocktail (Complete mini, Roche). Criterion 4%–15% polyaccrylamide gels (Bio-Rad, Hercules, CA) were loaded with 20 mg of total protein and the gel was run for 1.5 hours at 150V. The gel was transferred to PVDF membranes for Western analysis. Membranes were incubated in primary antibody for 36 hours. Primary antibodies used were Smooth-muscle myosin heavy chain (1:10, Leica, Bannockburn, IL), smoothelin (1:100, Milipore, Billerica, MA) and beta actin (1:5000, Santa Cruz Biotechnology, Santa Cruz, CA). Secondary antibodies were conjugated with infrared labels (1:15000, Licor, Lincoln, NE) and imaged with a Licor Odyssey reader (Licor, Lincoln, NE). Quantification was performed by densitometry analysis using Odyssey 3.0 software. Quantified values were compared using a 2-way ANOVA (patterning, ECM) and pairwise comparisons were done using Tukey tests.

ACKNOWLEDGEMENTS

This work was funded by the Defense Advanced Research Projects Agency PREVENT, through the Office of Naval Research, award number N66001-08-C-2036, the Nanoscale Science and Engineering Center of the

National Science Foundation under NSF award number PHY-0117795, the Harvard Materials Research Science and Engineering Center under NSF award number DMR-0213805, the NSF REU program under award number 1005022, and NIH grant 1 R01 HL079126-01A2 (K.K.P.).

REFERENCES

1. Chen CS, Mrksich M, Huang S, Whitesides GM, Ingber DE. Geometric control of cell life and death. Science. 1997;276:1425–1428 [PubMed: 9162012]
2. Parker KK, Brock AL, Brangwynne C, Mannix RJ, Wang N, Ostuni E, Geisse NA, Adams JC, Whitesides GM, Ingber DE. Directional control of lamellipodia extension by constraining cell shape and orienting cell tractional forces. Faseb J. 2002;16
3. Nelson CM, Jean RP, Tan JL, Liu WF, Sniadecki NJ, Spector AA, Chen CS. Emergent patterns of growth controlled by multicellular form and mechanics. Proc Natl Acad Sci U S A. 2005;102:11594–11599 [PubMed: 16049098]
4. Bray MA, Sheehy SP, Parker KK. Sarcomere alignment is regulated by myocyte shape. Cell Motil Cytoskeleton. 2008;65:641–651 [PubMed: 18561184]
5. Parker KK, Tan J, Chen CS, Tung L. Myofibrillar architecture in engineered cardiac myocytes. Circ Res. 2008;103:340–342 [PubMed: 18635822]
6. Bursac N, Parker KK, Iravanian S, Tung L. Cardiomyocyte cultures with controlled macroscopic anisotropy: A model for functional electrophysiological studies of cardiac muscle. Circ Res. 2002;91:e45–54 [PubMed: 12480825]
7. Rhodin JAG. Architecture of the vessel wall. In: Berne R, ed. Handbook of physiology. American Physiology Society; 1979.
8. Davies PF. Flow-mediated endothelial mechanotransduction. Physiological reviews. 1995;75:519–560 [PubMed: 7624393]
9. Tarbell JM, Weinbaum S, Kamm RD. Cellular fluid mechanics and mechanotransduction. Ann Biomed Eng. 2005;33:1719–1723 [PubMed: 16389519]
10. Davis MJ, Hill MA. Signaling mechanisms underlying the vascular myogenic response. Physiological reviews. 1999;79:387–423 [PubMed: 10221985]
11. Schubert R, Mulvany MJ. The myogenic response: Established facts and attractive hypotheses. Clin Sci (Lond). 1999;96:313–326 [PubMed: 10087237]
12. Owens GK, Kumar MS, Wamhoff BR. Molecular regulation of vascular smooth muscle cell differentiation in development and disease. Physiological reviews. 2004;84:767–801 [PubMed: 15269336]
13. Rensen SS, Doevendans PA, van Eys GJ. Regulation and characteristics of vascular smooth muscle cell phenotypic diversity. Neth Heart J. 2007;15:100–108 [PubMed: 17612668]
14. Mecham RP, Whitehouse LA, Wrenn DS, Parks WC, Griffin GL, Senior RM, Crouch EC, Stenmark KR, Voelkel NF. Smooth muscle-mediated connective tissue remodeling in pulmonary hypertension. Science. 1987;237:423–426 [PubMed: 3603030]
15. Libby P, Tanaka H. The molecular bases of restenosis. Prog Cardiovasc Dis. 1997;40:97–106 [PubMed: 9327826]
16. Yamaguchi-Okada M, Nishizawa S, Koide M, Nonaka Y. Biomechanical and phenotypic changes in the vasospastic canine basilar artery after subarachnoid hemorrhage. J Appl Physiol. 2005;99:2045–2052 [PubMed: 16051708]
17. Stegemann JP, Hong H, Nerem RM. Mechanical, biochemical, and extracellular matrix effects on vascular smooth muscle cell phenotype. J Appl Physiol. 2005;98:2321–2327 [PubMed: 15894540]
18. Qin H, Ishiwata T, Wang R, Kudo M, Yokoyama M, Naito Z, Asano G. Effects of extracellular matrix on phenotype modulation and mapk transduction of rat aortic smooth muscle cells in vitro. Exp Mol Pathol. 2000;69:79–90 [PubMed: 11001858]
19. Thyberg J, Hultgardh-Nilsson A. Fibronectin and the basement membrane components laminin and collagen type iv influence the phenotypic properties of subcultured rat aortic smooth muscle cells differently. Cell Tissue Res. 1994;276:263–271 [PubMed: 8020062]

20. Hedin U, Bottger BA, Forsberg E, Johansson S, Thyberg J. Diverse effects of fibronectin and laminin on phenotypic properties of cultured arterial smooth muscle cells. J Cell Biol. 1988;107:307–319 [PubMed: 2455726]
21. Peyton SR, Putnam AJ. Extracellular matrix rigidity governs smooth muscle cell motility in a biphasic fashion. J Cell Physiol. 2005;204:198–209 [PubMed: 15669099]
22. Li S, Lao J, Chen BP, Li YS, Zhao Y, Chu J, Chen KD, Tsou TC, Peck K, Chien S. Genomic analysis of smooth muscle cells in 3-dimensional collagen matrix. Faseb J. 2003;17:97–99 [PubMed: 12475912]
23. Kim BS, Nikolovski J, Bonadio J, Mooney DJ. Cyclic mechanical strain regulates the development of engineered smooth muscle tissue. Nat Biotechnol. 1999;17:979–983 [PubMed: 10504698]
24. Stringa E, Knauper V, Murphy G, Gavrilovic J. Collagen degradation and platelet-derived growth factor stimulate the migration of vascular smooth muscle cells. J Cell Sci. 2000;113 (Pt 11):2055–2064 [PubMed: 10806116]
25. Deaton RA, Su C, Valencia TG, Grant SR. Transforming growth factor-beta1-induced expression of smooth muscle marker genes involves activation of pkn and p38 mapk. J Biol Chem. 2005;280:31172–31181 [PubMed: 15980430]
26. Thakar RG, Cheng Q, Patel S, Chu J, Nasir M, Liepmann D, Komvopoulos K, Li S. Cell-shape regulation of smooth muscle cell proliferation. Biophys J. 2009;96:3423–3432 [PubMed: 19383485]
27. Williams C, Brown XQ, Bartolak-Suki E, Ma H, Chilkoti A, Wong JY. The use of micropatterning to control smooth muscle myosin heavy chain expression and limit the response to transforming growth factor beta1 in vascular smooth muscle cells. Biomaterials. 2011;32:410–418 [PubMed: 20858564]
28. Feinberg AW, Feigel A, Shevkoplyas SS, Sheehy S, Whitesides GM, Parker KK. Muscular thin films for building actuators and powering devices. Science. 2007;317:1366–1370 [PubMed: 17823347]
29. Alford PW, Feinberg AW, Sheehy SP, Parker KK. Biohybrid thin films for measuring contractility in engineered cardiovascular muscle. Biomaterials. 2010;31:3613–3621 [PubMed: 20149449]
30. Alford PW, Dabiri BE, Goss JA, Hemphill MA, Brigham MD, Parker KK. Blast-induced phenotypic switching in cerebral vasospasm. Proceedings of the National Academy of Sciences of the United States of America. 2011;108:12705–12710 [PubMed: 21765001]
31. Cao Y, Poon YF, Feng J, Rayatpisheh S, Chan V, Chan-Park MB. Regulating orientation and phenotype of primary vascular smooth muscle cells by biodegradable films patterned with arrays of microchannels and discontinuous microwalls. Biomaterials. 2010;31:6228–6238 [PubMed: 20537704]
32. Vicente-Manzanares M, Choi CK, Horwitz AR. Integrins in cell migration--the actin connection. J Cell Sci. 2009;122:199–206 [PubMed: 19118212]
33. Reilly GC, Engler AJ. Intrinsic extracellular matrix properties regulate stem cell differentiation. J Biomech. 2010;43:55–62 [PubMed: 19800626]
34. Volfson D, Cookson S, Hasty J, Tsimring LS. Biomechanical ordering of dense cell populations. Proceedings of the National Academy of Sciences of the United States of America. 2008;105:15346–15351 [PubMed: 18832176]
35. Bray MA, Adams WJ, Geisse NA, Feinberg AW, Sheehy SP, Parker KK. Nuclear morphology and deformation in engineered cardiac myocytes and tissues. Biomaterials. 2010;31:5143–5150 [PubMed: 20382423]
36. Schwartz SM, Campbell GR, Campbell JH. Replication of smooth muscle cells in vascular disease. Circ Res. 1986;58:427–444 [PubMed: 3516443]
37. Pauly RR, Bilato C, Cheng L, Monticone R, Crow MT. Vascular smooth muscle cell cultures. Methods Cell Biol. 1997;52:133–154 [PubMed: 9379948]
38. Ichii T, Koyama H, Tanaka S, Kim S, Shioi A, Okuno Y, Raines EW, Iwao H, Otani S, Nishizawa Y. Fibrillar collagen specifically regulates human vascular smooth muscle cell genes involved in cellular responses and the pericellular matrix environment. Circ Res. 2001;88:460–467 [PubMed: 11249868]

39. Delfino A, Stergiopulos N, Moore JE Jr., Meister JJ. Residual strain effects on the stress field in a thick wall finite element model of the human carotid bifurcation. J Biomech. 1997;30:777–786 [PubMed: 9239562]
40. Alford PW, Taber LA. Computational study of growth and remodelling in the aortic arch. Comput Methods Biomech Biomed Engin. 2008;11:525–538 [PubMed: 18792831]
41. Alford PW, Humphrey JD, Taber LA. Growth and remodeling in a thick-walled artery model: Effects of spatial variations in wall constituents. Biomech Model Mechanobiol. 2008;7:245–262 [PubMed: 17786493]
42. Schmid H, Watton PN, Maurer MM, Wimmer J, Winkler P, Wang YK, Rohrle O, Itskov M. Impact of transmural heterogeneities on arterial adaptation. Biomech Model Mechanobiol. 2010;9:295–315 [PubMed: 19943177]
43. Wagenseil JE, Mecham RP. Vascular extracellular matrix and arterial mechanics. Physiological reviews. 2009;89:957–989 [PubMed: 19584318]
44. Grosberg A, Kuo PL, Guo CL, Geisse NA, Bray MA, Adams WJ, Sheehy SP, Parker KK. Self-organization of muscle cell structure and function. PLoS Comput Biol. 2011;7:e1001088 [PubMed: 21390276]
45. Gerdes AM, Kellerman SE, Moore JA, Muffly KE, Clark LC, Reaves PY, Malec KB, McKeown PP, Schocken DD. Structural remodeling of cardiac myocytes in patients with ischemic cardiomyopathy. Circulation. 1992;86:426–430 [PubMed: 1638711]
46. Gerdes AM, Capasso JM. Structural remodeling and mechanical dysfunction of cardiac myocytes in heart-failure. J Mol Cell Cardiol. 1995;27:849–856 [PubMed: 7602601]
47. Maniotis AJ, Chen CS, Ingber DE. Demonstration of mechanical connections between integrins cytoskeletal filaments, and nucleoplasm that stabilize nuclear structure. Proceedings of the National Academy of Sciences of the United States of America. 1997;94:849–854 [PubMed: 9023345]
48. Dahl KN, Ribeiro AJ, Lammerding J. Nuclear shape, mechanics, and mechanotransduction. Circ Res. 2008;102:1307–1318 [PubMed: 18535268]
49. Sims JR, Karp S, Ingber DE. Altering the cellular mechanical force balance results in integrated changes in cell, cytoskeletal and nuclear shape. J Cell Sci. 1992;103 (Pt 4):1215–1222 [PubMed: 1487498]
50. Wang N, Tytell JD, Ingber DE. Mechanotransduction at a distance: Mechanically coupling the extracellular matrix with the nucleus. Nat Rev Mol Cell Biol. 2009;10:75–82 [PubMed: 19197334]
51. Conte MS. The ideal small arterial substitute: A search for the holy grail?Faseb J. 1998;12:43–45 [PubMed: 9438409]
52. Niklason LE, Gao J, Abbott WM, Hirschi KK, Houser S, Marini R, Langer R. Functional arteries grown in vitro. Science. 1999;284:489–493 [PubMed: 10205057]
53. L'Heureux N, Stoclet J-C, Auger FA, Lagaud GJ-L, Germain L, Andriantsitohaina R. A human tissue-engineered vascular media: A new model for pharmacological studies of contractile responses. FASEB J. 2001;15:515–524 [PubMed: 11156967]
54. Isenberg BC, Williams C, Tranquillo RT. Small-diameter artificial arteries engineered in vitro. Circ Res. 2006;98:25–35 [PubMed: 16397155]
55. Yamamoto M, Yamamoto K, Noumura T. Type i collagen promotes modulation of cultured rabbit arterial smooth muscle cells from a contractile to a synthetic phenotype. Exp Cell Res. 1993;204:121–129 [PubMed: 8416790]
56. Han M, Wen J-K, Zheng B, Cheng Y, Zhang C. Serum deprivation results in redifferentiation of human umbilical vascular smooth muscle cells. Am J Physiol Cell Physiol. 2006;291:C50–58 [PubMed: 16467401]

Insight, Innovation and Integration

Vascular tissue structure and contractile function vary from vessel to vessel, and maladaptive changes in arterial architecture may play a role in vascular disease progression. To understand the role of arterial structure in determining its function, we microfabricated tissues of vascular smooth muscle with differing tissue and cell-level architecture and employed vascular muscular thin film technology to measure their dynamic stress generation during contraction. Interestingly, we found that cellular and nuclear architecture more strongly correlate with contractile function than does expression of traditionally measured contractile markers. This novel finding suggests that smooth muscle cell structure within a tissue plays a significant role in both functional and dysfunctional vascular regulation.

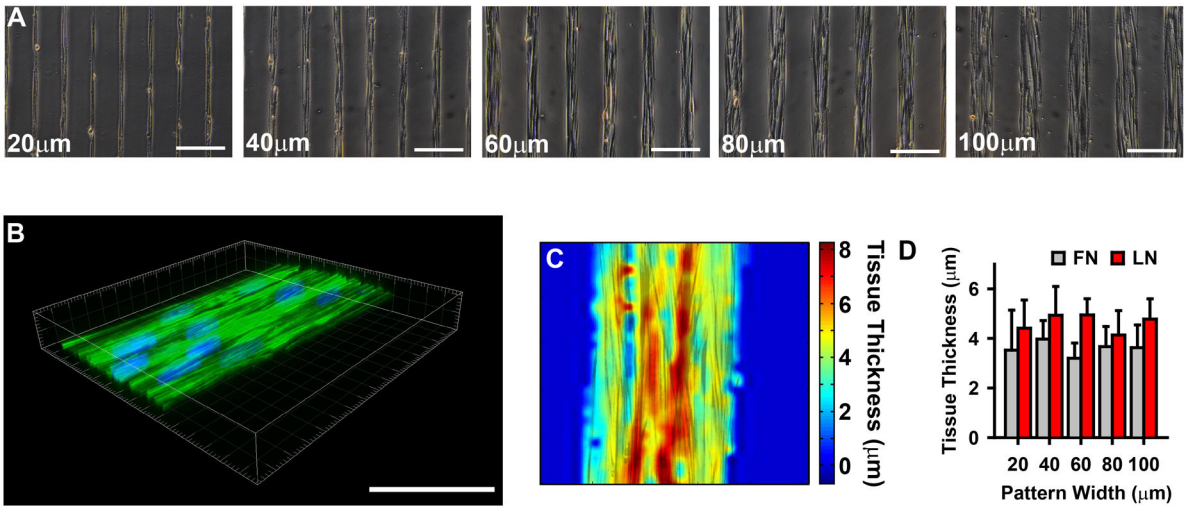

Figure 1:

Microcontact printing used to provide spatial cues for vascular tissue self-organization. (A) Phase contrast images of VSMCs micropatterned into thin tissue lines of varying widths, indicated in each image, separated by 100 μm gaps. (scale bars =200 μm). (B) 3-D confocal image of 100 μm wide patterned VSMC tissue. (Green: f-actin, Blue: nuclei). Scale bar 100 μm. (C) Thickness map of tissue in B, using f-actin staining. (D) Tissue thickness as a function of pattern width and ECM (fibronectin (FN) and laminin (LN)) substrate (mean +/− SD).

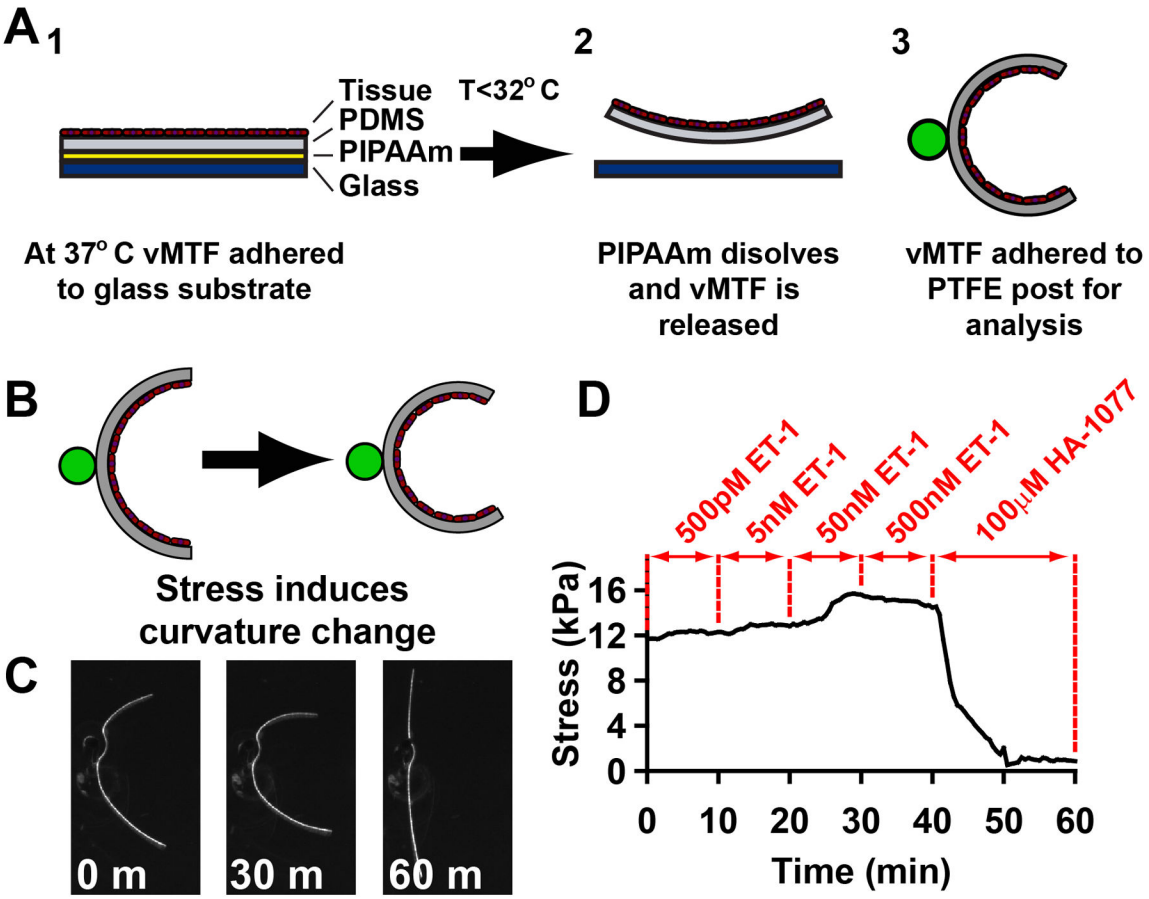

Figure 2:

Vascular muscular thin film (vMTF) construction and experimental methods. (A) Schematic representation of vMTF method. (B) Curvature of vascular muscular thin films was used to calculate change in tissue stress. (C) Example images from one vMTF experiment, pre ET-1 treatment (0 minutes), after 50 nM ET-1 stimulation (30 minutes) and following HA-1077 treatment (60 minutes). (D) Typical temporal apparent stress evolution for serial stimulation of vMTF with increasing doses of endothelin-1 followed by HA-1077.

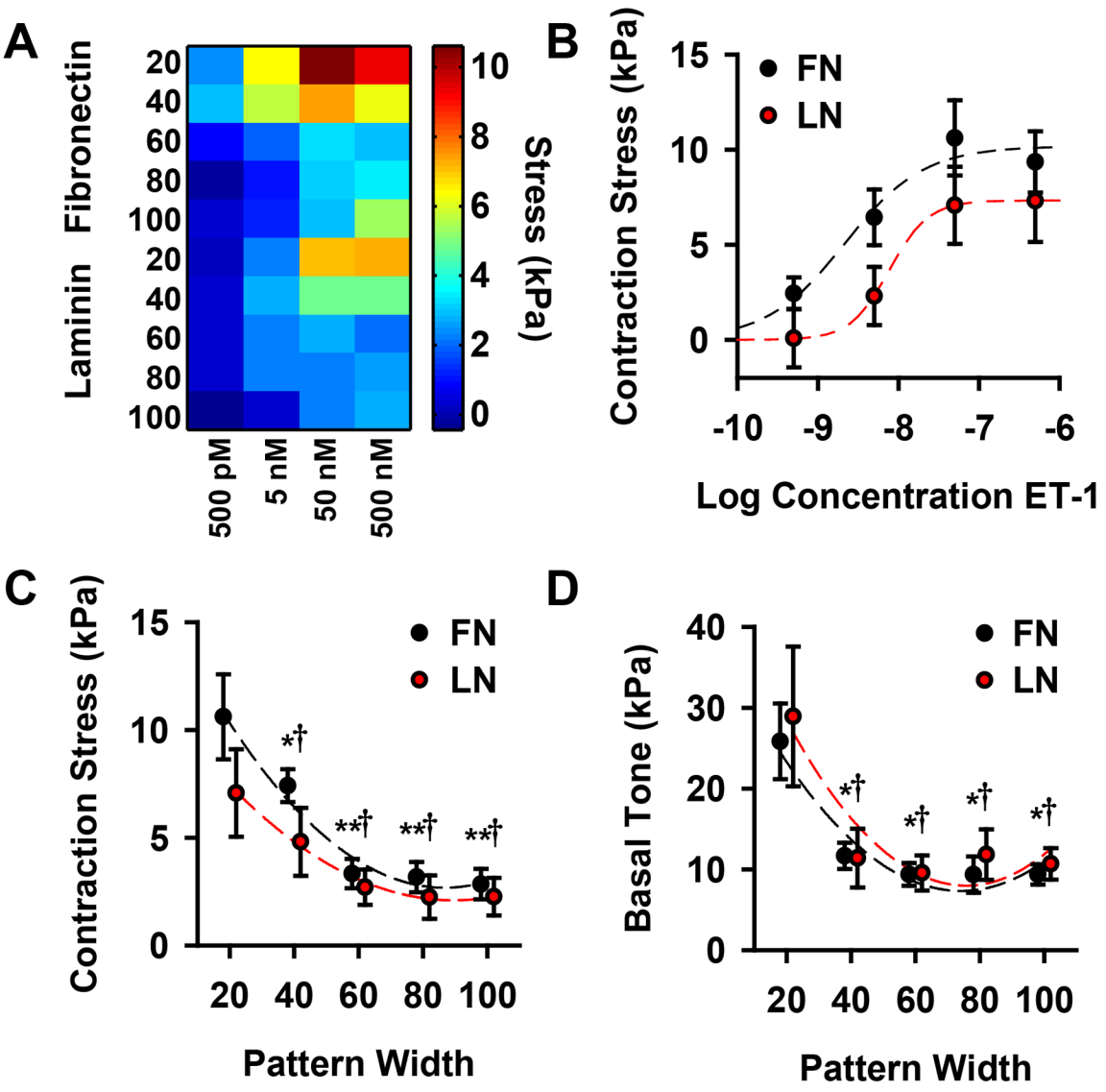

Figure 3:

Vascular tissue structure influences functional contractile output. (A) Heat map representing dose-response behavior of all tissue types, patterned on fibronectin (FN) and laminin (LN). (B) Typical sigmoidal dose-response curves for 20 μm wide lines patterned on both fibronectin and laminin. (C) Tissue contraction induced by 50 nM ET-1 stimulation for all tissues. (D) Basal contractile tone for all tissues. (for F,G; * = statistically different from 20 μm FN tissue, †=statistically different from 20 μm LN tissue, **=statistically different from both 20 μm and 40 μm FN tissue, $p<0.05$). All plots: mean +/− SEM.

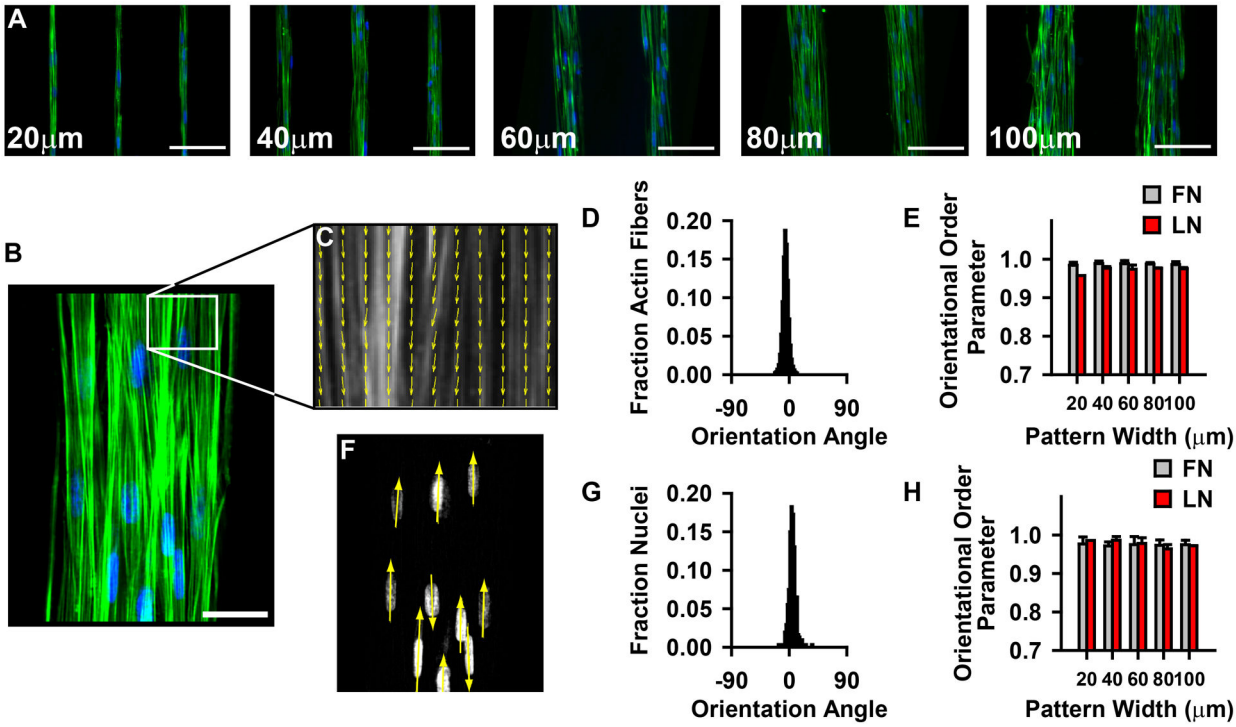

Figure 4:

Constrained tissue structure does not significantly alter subcellular organization. (A–B) Phalloidin and DAPI stained images of patterned tissues. (Green: f-actin, Blue: nuclei). (A) scale bar = 100 μm (B) scale bar = 50 μm. (C) Actin orientation map for a representative region of the tissue in (B). (D) Histogram of actin orientation angles in 100 μm wide tissues. (E) F-actin orientational order parameter for all tissue patterns. (FN: fibronectin, LN: laminin; mean +/− sd) (F) Nuclear orienatation map for nuclei in (B). (G) Histogram of nuclear orientation in 100 μm wide tissues. (H) Nuclear orienational order parameter for all tissue patterns. (FN: fibronectin, LN: laminin; mean +/− sd)

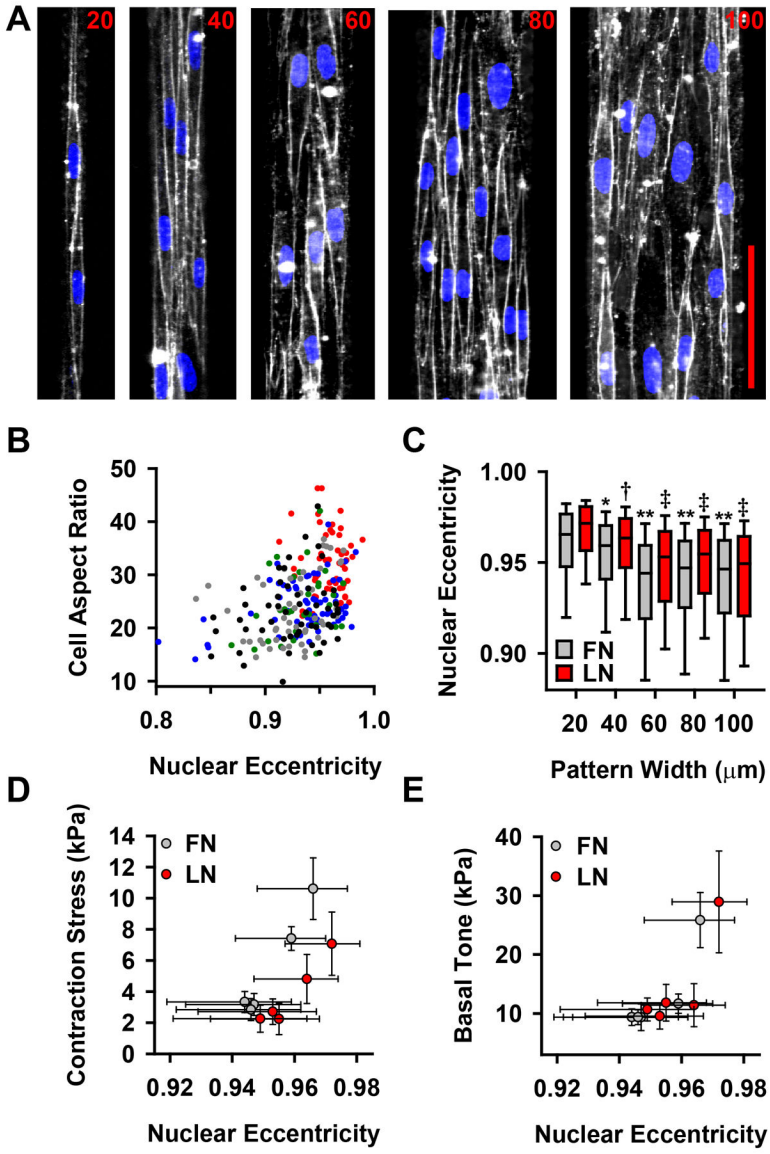

Figure 5:

Cell and nuclear morphology correlate with VSMC functional output. (A) Di-8 membrane (white) and DAPI nuclear (blue) stained micropatterned vascular tissues. scale bar=100 μm (B) Correlation between cell aspect ratio and nuclear eccentricity. Each circle represents a single cell. Color indicates tissue width of measured cell (red: 20 μm, blue: 40 μm, green: 60 μm, gray: 80 μm, black: 100 μm). Pearson correlation of cell aspect ratio and nuclear eccentricity: r=0.346, p=1.66e-7. (C) Nuclear eccentricity for patterned vascular tissues (* = statistically different from 20 μm FN tissue, †=statistically different from 20 μm LN tissue, **=statistically different from both 20 μm and 40 μm FN tissue, ‡ = statistically different from both 20 μm and 40 μm LN tissue, p<0.05) box: 25–75%, error bars: 10–90% (D) Nuclear eccentricity correlates with contraction stress (see Fig 3C) following stimulation with 50 nM ET-1 (Pearson correlation: r=0.748, p=0.013). (E) Nuclear eccentricity correlates with basal contractile tone (see Fig 3D) (Pearson correlation:

r=0.823, p=0.008). (D–E) Error bars: x: 25–75% (from (C)), y: SEM (from Fig 3 C,D). Reported p values for Pearson correlations are two-tailed, demonstrating that the correlation is significantly different from zero.

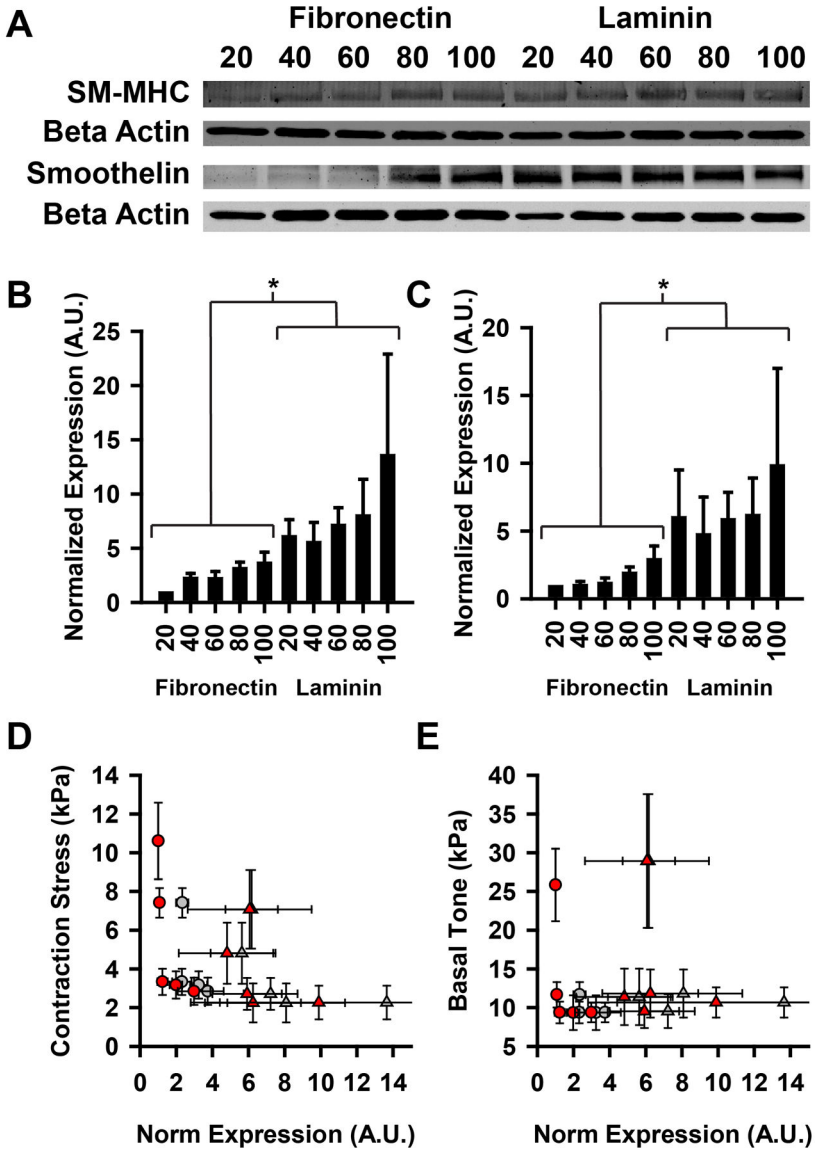

Figure 6:

Contractile phenotype protein expression does not correlate with contractile output. (A) Example western blot for contractile markers smooth muscle myosin heavy chain and smoothelin. (B) Quantified expression of SM-MHC. *=FN and LN statistically different from one another ($p<0.05$). (C) Quantified expression of smoothelin. *=FN and LN statistically different from one another ($p<0.05$). (D–E) Contractile stress and basal tone plotted against quantified expression of SM-MHC and smoothelin. (circles: FN, triangles: LN, gray: SM-MHC, red: smoothelin) For correlation analyses, FN and LN data points were pooled and treated as one group. (D) Contraction stress. (Pearson correlation: r, p). SM-MHC: (−0.553, 0.975), smoothelin (−0.475, 0.166) (E) Basal tone. (Pearson correlation: r, p). SM-MHC: (−0.179,0.621), smoothelin: (−0.031, 0.933). All error bars mean +/− SEM. (D-E) Reported p value is two-tailed, demonstrating that the correlations are not significantly different from zero.